Strong Cosserat Elasticity in a Transversely Isotropic Polymer Lattice

Z. Rueger and R. S. Lakes[*]

Department of Engineering Physics, Department of Materials Science, University of Wisconsin, Madison, Wisconsin 53706-1687, USA

Large size effects are experimentally measured in lattices of triangular unit cells: about a factor of 36 in torsion rigidity and 29 in bending rigidity. This nonclassical phenomenon is consistent with Cosserat elasticity, which allows for the rotation of points and distributed moments in addition to the translation of points and force stress of classical elasticity. The Cosserat characteristic length for torsion is $\ell_t = 9.4$ mm; for bending, it is $\ell_b = 8.8$ mm; these values are comparable to the cell size. Nonclassical effects are much stronger than in stretch-dominated lattices with uniform straight ribs. The lattice structure provides a path to the attainment of arbitrarily large effects.

Continuum theories of elasticity are widely used for representing materials with microstructure, including composites and lattice "metamaterials," as continuous media. The currently accepted classical theory permits the Poisson ratio in isotropic materials to range from -1 to $1/2$ and incorporates two independent elastic constants. A theory with less freedom was tried: The uniconstant theory of elasticity, developed by Navier [1], incorporates only one elastic constant, a modulus, and was based on an assumption that forces acted along the lines joining pairs of atoms and were proportional to changes in the distance between them. Navier's theory predicted a Poisson ratio of $1/4$ for all isotropic materials and was abandoned when experiments demonstrated a range of Poisson ratios, so the current classical theory was adopted. The Cosserat theory [2] (with inertia terms called micropolar [3]) has more freedom than classical elasticity; it incorporates a local rotation of points and a couple stress (torque per unit area) as well as the translation of points and force stress of classical elasticity. The Cosserat theory of elasticity has six independent isotropic elastic constants and even more constants if the material is anisotropic. In contrast to classical elasticity, Cosserat elasticity incorporates a characteristic length scale in the continuum; the solid becomes sensitive to strain gradients, and, hence, has a nonlocal aspect, and can support an asymmetric stress.

Classical elasticity is entirely adequate for macroscopic specimens in which the structure size is many orders of magnitude smaller than the experimental size scale; macroscopic scale tests for Cosserat effects in aluminum revealed classical behavior [4]. Nonclassical elastic effects are expected if the ratio of structural to experimental length scale is non-negligible. At the atomic scale, noncentral forces are associated with moments such as those between dipoles; these moments can be subsumed in a Cosserat analysis. The dispersion of waves of a length a small multiple of the lattice spacing was used to infer Cosserat behavior in diamond crystals [5]; the inferred characteristic length was about 0.2 nm. More recently, classical elasticity [6] was predicted to break down in crystalline materials in the length scale range of 1–10 nm. In chiral cholesteric elastomers [7], the characteristic length was predicted to be on the order of 10 nm. These length scales are on the order of the structure size. Cosserat-type freedom is not limited to elasticity; it can occur in other physical properties. Piezoelectric materials are known to exhibit nonclassical sensitivity to gradients [8], interpreted via a nonlocal concept [9]. The characteristic length, governed by the spacing of ions in the lattice, is enhanced in ferroelectrics, so that effects were observed in layers several micrometers thick. Such materials in recent studies have been called flexoelectric [10].

A larger characteristic length is to be expected in materials with larger structural length scales. This is not a sufficient condition; the specific nature of the structure is pertinent as well. The Cosserat couple stress arises from the superposition of bending and twisting moments transmitted by the structural elements in materials. The Cosserat local rotation corresponds to the rotation of the structural elements. Forces and moments are also considered in the classical analyses of foam [11] in which classical elastic moduli were determined; effects of rotation gradients were not considered. Lattices with straight elastic ribs were analyzed via theoretical homogenization [12–14] as Cosserat solids. Such lattices, despite their structure, are nearly classical; the Cosserat characteristic lengths are much smaller than their cell sizes. The reason is that these structures are stretch dominated: The effects of rib extension greatly exceed the effects of rib bending and torsion. Rib extension in such structures governs the force stress and, hence, the classical elastic moduli; rib bending and torsion transmits moments corresponding to the Cosserat couple stress. The distributed Cosserat moments are minimal in comparison with the forces, so the characteristic length is small compared with the cell size in such lattices.

A composite containing round aluminum beads in an epoxy matrix was tested experimentally for Cosserat effects and was found to be classical [15]. Indeed, composites containing stiff spheres were shown by a homogenization analysis to have characteristic lengths of zero [16]. A dense closed cell polymer foam exhibited Cosserat effects; the characteristic length was comparable to the cell size (the largest cells had a diameter of 0.15 mm), but size effects (see below) were only about a factor of 1.3 as a result of weak coupling [17]. Rotational waves of the sort anticipated in Cosserat elasticity were observed in a noncohesive granular assembly of metal spheres [18]. A value of κ (defined below) was inferred, but characteristic lengths were not obtained; indeed, the granular assembly was predicted to have rotation gradient sensitivity terms α, β, and γ equal to zero and, hence, zero characteristic length; as with composites with hard spheres, this is a degenerate case.

Lattices of the type presented in this Letter exhibit strong nonclassical effects consistent with Cosserat elasticity; the design provides a path to achieving arbitrarily large Cosserat effects.

In Cosserat elasticity, the stress σ_{jk} can be asymmetric. The resulting moment is balanced by a couple stress, m_{jk}. The antisymmetric part of the stress is related to local rotations: $\sigma_{jk}^{\text{antisym}} = \kappa e_{jkm}(r_m - \phi_m)$, in which κ is an elastic constant, ϕ_m is the rotation of points, called a microrotation, e_{jkm} is the permutation symbol, and $r_k = \frac{1}{2}e_{klm}u_{m,l}$ is the macrorotation based on the antisymmetric part of gradient of displacement u_i. The constitutive equations for linear isotropic Cosserat elasticity [3] are as follows:

$$\sigma_{ij} = 2G\epsilon_{ij} + \lambda\epsilon_{kk}\delta_{ij} + \kappa e_{ijk}(r_k - \phi_k), \quad (1)$$

$$m_{ij} = \alpha\phi_{k,k}\delta_{ij} + \beta\phi_{i,j} + \gamma\phi_{j,i}. \quad (2)$$

There are six independent elastic constants for an isotropic Cosserat solid. Constants λ and G have the same meaning as in classical elasticity; α, β, and γ provide sensitivity to rotation gradients, and κ quantifies the coupling between fields. Technical constants derived from these elastic constants are beneficial for physical insight and are as follows: Young's modulus $E = [G(3\lambda + 2G)/(\lambda + G)]$, shear modulus G, Poisson ratio $\nu = [\lambda/2(\lambda + G)]$, characteristic length, torsion $\ell_t = \sqrt{[(\beta + \gamma)/(2G)]}$, characteristic length, bending $\ell_b = \sqrt{[\gamma/(4G)]}$, coupling number $N = \sqrt{[\kappa/(2G + \kappa)]}$, and polar ratio $\Psi = [(\beta + \gamma)/(\alpha + \beta + \gamma)]$. This is a generalization of the extraction of technical constants from tensorial ones in classical elasticity.

There are several key consequences of Cosserat elasticity which differ from classical predictions. Circular holes exhibit a lower stress concentration factor than expected classically, and small holes exhibit less stress concentration than larger ones [19]. A characteristic of Cosserat elasticity pertinent to the research presented in this Letter is the

(a) 3D printed rib structure.
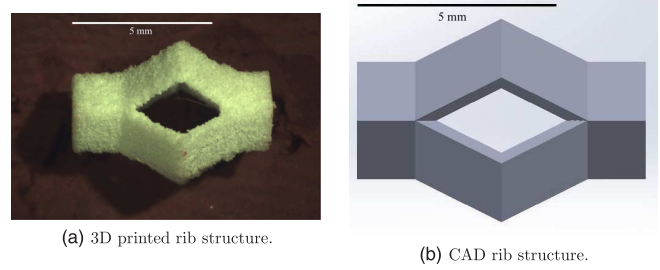
(b) CAD rib structure.

FIG. 1. 3D printed rib structure vs idealized drawing. Scale bar, 5 mm.

prediction of a size effect in the torsion [15] and bending [20] of circular cylinders of Cosserat elastic materials. These size effects manifest as slender cylinders appearing stiffer than predicted classically. The lattices considered in this Letter were developed to achieve strong Cosserat effects by decoupling the rib rigidity in torsion and bending from its rigidity in extension. This maximizes sensitivity to the rotation gradient. These lattices were embodied via selective laser sintering, an additive manufacturing technique. The lattice was modeled in SolidWorks and was converted to stereolithography (STL) format for export to 3D printing. Specimens were printed by a 3D Systems sPro 60 HD-HS printer. The parent material was a polyamide polymer equivalent to nylon 12. Each rib element (Fig. 1) consists of square section tubular segments with a portion that approximates a Sarrus linkage. The ideal Sarrus linkage contains hinged elements and offers zero resistance to axial compression but resists torsion. The measured effective Young's modulus in bending of one rib element was 281 MPa; in compression, it was 14 MPa; for a solid rod, these moduli would be equal. The torsional modulus was 387 MPa. The ribs, though not hinged, therefore resist torsion and bending to a much greater extent than compression. This rib design was created to be sensitive to gradients and thus demonstrate large size effects when used to construct 3D structures. Each rib connects with its neighbors via hexagonal nodes shown in Fig. 2. The lattice comprised of these ribs consists of triangular prism unit cells of which the side length of the triangular bases was 10.5 mm and the height was 9.0 mm. The lattice density was 0.16 g/cm³.

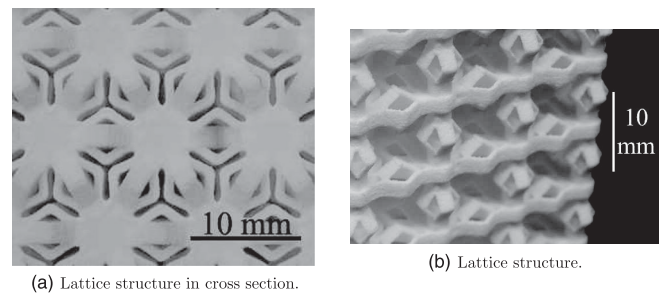(a) Lattice structure in cross section.

(b) Lattice structure.

FIG. 2. Cross section and side view of 3D printed lattice structure. Scale bar, 10 mm.

Cosserat effects were probed by measuring the size dependence of rigidity at a constant frequency. This protocol provides sensitivity to spatial gradients; it is insensitive to time derivatives, because all the experiments were done at the same frequency. By contrast, in wave methods, a change in the wavelength is accompanied by a change in the frequency. Therefore, wave dispersion due to viscoelastic damping cannot be distinguished from dispersion due to the sensitivity to spatial gradients. Five structures of increasing size, but the same aspect ratio, were printed. Specimens had complete cells with no partial cells; this was done by making cross section shapes aligned with the symmetry axes. All sections were hexagonal except the smallest, which was triangular. Equivalent circles were inscribed for interpretation. The specimens, from smallest to largest, were composed of the following number of unit cells in cross section by height: 1×3, 6×7, 24×13, 54×19, and 96×26.

These specimens were tested for torsional and bending rigidities using a broadband viscoelastic spectrometer (BVS) [21]. This apparatus uses a pair of Helmholtz coils to apply a torque of controllable direction to the specimen via a magnet attached to the base via a ceramic stalk and cement. The magnet was calibrated in the BVS using a lock-in amplifier. A mirror was glued to the specimen's base edge. To measure displacement, the beam of a semiconductor laser was reflected off this mirror and directed to a silicon light detector. The light detector was calibrated by moving it a known distance, via the calibration stage, and measuring the output voltage. A calibration curve was generated, and the change in output voltage per change in position was used as the beam position calibration constant (V/μm).

A sinusoidal signal with a frequency of 1 Hz was input to the torsion Helmholtz coil. The same frequency was used for all specimen sizes to decouple viscoelastic effects from the size effects being probed. The resulting torque vs angular displacement signals were displayed as a Lissajous figure on an oscilloscope; the modulus and viscoelastic damping of the structures were then calculated. To measure bending moduli, the orthogonal bending Helmholtz coil was used, and the light detector was switched to measure vertical displacement. The calibration constant for the light detector was determined as before, and the magnet's calibration constant for bending was used in calculations.

Compression tests were conducted using a screw-driven test frame to ascertain the Young's modulus of the specimens in the absence of macroscopic gradients of strain or rotation as well as to measure the Poisson ratio. Anisotropy of the modulus was probed via propagation in different directions of acoustic waves of a wavelength much larger than the cell size.

Size effects in torsion were interpreted using the following exact solution for a Cosserat elastic circular rod of radius r with Ω as the ratio of structural rigidity to its classical counterpart [15]:

$$\Omega = \left(1 + 6\left(\frac{\ell_t}{r}\right)^2\right)\left(\frac{1 - \frac{4}{3}\Psi\chi}{1 - \Psi\chi}\right), \qquad (3)$$

in which $\chi = I_1(pr)/prI_0(pr)$, $p^2 = 2\kappa/(\alpha + \beta + \gamma)$, and I_0 and I_1 are modified Bessel functions of the first kind. Classical torsional rigidity is $(M/\theta) = G[(\pi/2)r^4]$. G is the true shear modulus in the absence of gradients, M is the applied moment, and θ is the angular displacement per length.

The shear modulus G, characteristic length of torsion ℓ_t, and the coupling number N were found by fitting Eq. (3) to the full set of experimental data using MATLAB. Ψ was determined from the behavior of the data near the origin.

For bending, the classical rigidity is $(M/\theta) = E[(\pi/4)r^4]$. The exact expression of the rigidity ratio for the bending of a Cosserat elastic circular rod of radius r is

$$\Omega = 1 + 8\left(\frac{\ell_b}{r}\right)^2 \frac{\left[1 - \left(\frac{\beta}{\gamma}\right)^2\right]}{(1 + \nu)}$$
$$+ \frac{8N^2}{(1+\nu)}\left(\frac{\left(\frac{\beta}{\gamma} + \nu\right)^2}{\zeta(\delta r) + 8N^2(1 - \nu)}\right), \qquad (4)$$

in which $\delta = N/\ell_b$ and $\zeta(\delta r) = (\delta r)^2(\{(\delta r)I_0[(\delta r)] - I_1[(\delta r)]\}/[(\delta r)I_0(\delta r) - 2I_1(\delta r)])$. The Young's modulus E and Poisson ratio ν were determined from compression testing, while ℓ_b, β/γ, and N were determined from fitting the full set of experimental data with Eq. (4).

Results for torsion size effect studies are shown in Fig. 3. Viscoelastic dispersion of the modulus cannot obtrude in the interpretation, because all the experiments were conducted at 1 Hz.
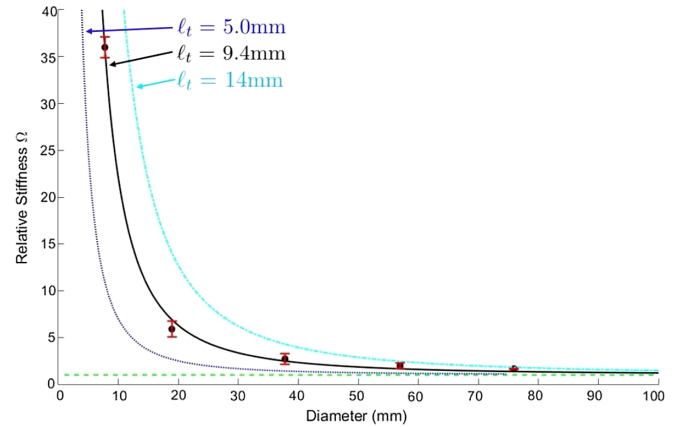

FIG. 3. Size effects for lattice specimens in torsion. Points are experimental. The black curve is theoretical for best fit $G = 1.1$ MPa, $\ell_t = 9.4$ mm, $N = 1$, and $\Psi = 1.0$. Blue and cyan curves illustrate theoretical predictions for $\ell_t = 5.0$ and 14 mm, respectively. Classical elasticity ($\ell_t = 0$) predicts constant $\Omega = 1$ independent of the diameter, which is indicated by the green horizontal dashed line.

For torsion, $G = 1.1$ MPa, $\ell_t = 9.4$ mm, and $N = 0.999$. Error bars shown were calculated from noise in the signal and from uncertainties in specimen dimensions. The mean absolute percent deviation between experimental results and the Cosserat prediction was 12%, while the root-mean-square deviation (RMSD) was 0.50. The increase in relative stiffness did not roll off near the origin; therefore, $\Psi < 1.5$. Results are consistent with $\Psi = 1$ but are not very sensitive to Ψ in this regime. The maximum size effect in torsion was $\Omega = 36$, corresponding to a 3500% deviation from the classical prediction. The asymptotic value of G was located via a curve fit. The characteristic length is comparable to the structure cell size.

The results of bending size effect studies are shown in Fig. 4, in which $E = 3.14$ MPa, $\nu = 0.05$, $\ell_b = 9.1$ mm, $\beta/\gamma = 0.5$, and $N = 0.99$. The mean absolute percent deviation between the experimental results and Cosserat prediction was 14%, while the RMSD was 0.58. The asymptotic value for E is based on the average compression modulus corrected for the difference in the frequency (0.04 vs 1 Hz) via dispersion inferred from observed damping tan $\delta \approx 0.05$. In compression, there is no strain gradient. Similarly, the Poisson ratio is the average based on compression. The maximum size effect in bending was $\Omega = 29.4$, corresponding to a 2843% deviation from the classical prediction.

It is concluded that the response follows Cosserat elasticity and not classical elasticity and that the Cosserat characteristic length is comparable to the cell size. Size effects are large in magnitude.

Pulsed acoustic wave measurements at 60° intervals in the transverse plane and in the longitudinal direction revealed the lattice material to exhibit elastic transverse isotropy. The longitudinal modulus was lower than the transverse by a factor of 1.3; the lattice does not deviate
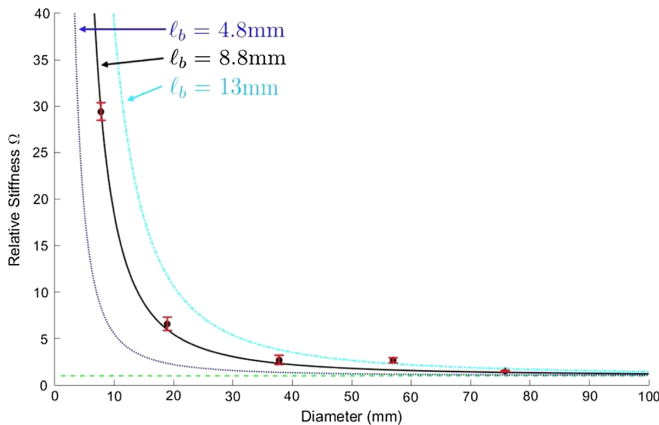

FIG. 4. Size effects for lattice specimens in bending. Points are experimental. The black curve is theoretical for best fit $E = 3.14$ MPa, $\nu = 0.05$, $\ell_b = 8.8$ mm, $\beta/\gamma = 0.5$, and $N = 0.99$. Blue and cyan curves illustrate theoretical predictions for $\ell_b = 4.8$ and 13 mm, respectively. Classical elasticity predicts constant $\Omega = 1$ independent of the diameter, which is indicated by the green horizontal dashed line.

much from isotropy. No analytical solutions for Cosserat elasticity are available for anisotropic rods. Therefore, the isotropic solutions discussed above were used for an interpretation, and the elastic constants were interpreted as technical constants. This is analogous to materials testing in classical elasticity, in which it is not always practical to incorporate a full anisotropic interpretation. Anisotropy is not a confounding variable, because size effects do not occur in classical elasticity even in the anisotropic case [22]. If need be, one may titrate the geometry of the structure to achieve elastic isotropy as has been done for negative Poisson ratio metal foams.

A wave cutoff frequency effect above 3 kHz was observed, but its interpretation is equivocal. A cutoff of waves can arise from structural resonance, from viscoelastic damping, or from both. In the present lattice, the wavelength at 3 kHz is about 5 times the cell size. Because the cells have a complex structure, such a wavelength may suffice for resonance. Attenuation based on a calculation from viscoelastic damping also suffices to significantly damp the waves above 3 kHz. Also, viscoelasticity contributes to wave dispersion, which in nondissipative solids could be used to infer Cosserat effects. So, for the present polymer lattice materials, the constant frequency size effect approach used here provides an unambiguous interpretation, in contrast to wave methods. Periodic crystal lattices of atoms [23] with minimal attenuation, by contrast, are amenable to wave methods.

As for further comparisons, in 2D chiral honeycomb lattices analyzed as Cosserat continua, the Cosserat characteristic lengths are similar to the cell size [24], and the Cosserat coupling number N approaches its upper limit of 1. Experiments on low-density open cell polymer foams disclose substantial size effects Ω up to a factor of 6.5 [25] and up to a factor of 12 [26] in negative Poisson ratio foam [27]. The characteristic length exceeded the cell size in both foams, but foams were much more compliant ($E = 91$ kPa for normal foam and 25 kPa for negative Poisson ratio foam) than the present lattices (3.14 MPa).

In contrast to foams, the present lattice structure provides a path to the attainment of arbitrarily large effects: The Sarrus-type rib segments can be made more slender, in view of future improvements in 3D printing. Bend-dominated behavior appears to be a necessary but not sufficient condition for strong Cosserat effects in cellular solids such as lattices and foams. Bend-dominated behavior refers to rib deformation that occurs primarily in bending rather than compression or axial stretch. By contrast, stretch-dominated lattice structures with straight uniform ribs are predicted to exhibit very weak Cosserat effects [12–14]. Other lattice "metamaterials" for high strength [28] made by 3D printing [29] have been treated as classically elastic in the absence of gradients but can be expected to exhibit Cosserat freedom, similarly lattice "metamaterials" with a controllable Hall coefficient [30].

In summary, large size effects are observed in the bending and torsion of designed lattices of triangular prismatic unit cells. The size effects are inconsistent with classical elasticity but are consistent with Cosserat elasticity. Other theories of elasticity with more degrees of freedom, such as those incorporated in the micromorphic or Mindlin microstructure theory [31] or microstretch elasticity [32], are not excluded; they are not necessary for the present observations.

*Corresponding author.
lakes@engr.wisc.edu

[1] S. P. Timoshenko, *History of Strength of Materials* (Dover Publications, New York, 1983).

[2] E. Cosserat and F. Cosserat, *Theorie des Corps Deformables* (Hermann et Fils, Paris, 1909).

[3] A. C. Eringen, in *Fracture*, edited by H. Liebowitz (Academic Press, New York, 1968), Vol. 1, pp. 621–729.

[4] J. Schijve, Note on couple stresses, J. Mech. Phys. Solids **14**, 113 (1966).

[5] S. Minagawa, K. Arakawa, and M. Yamada, Diamond crystals as Cosserat continua with constrained rotation, Phys. Status Solidi A **57**, 713 (1980).

[6] R. Maranganti and P. Sharma, Length Scales at Which Classical Elasticity Breaks Down for Various Materials, Phys. Rev. Lett. **98**, 195504 (2007).

[7] M. Warner, E. M. Terentjev, R. B. Meyer, and Y. Mao, Untwisting of a Cholesteric Elastomer by a Mechanical Field, Phys. Rev. Lett. **85**, 2320 (2000).

[8] E. V. Bursian and O. I. Zaikovskii, Changes in the curvature of a ferroelectric film due to polarization, Sov. Phys. Solid State **10**, 1121 (1968).

[9] E. V. Bursian and N. N. Trunov, Nonlocal piezoelectric effect, Sov. Phys. Solid State **16**, 760 (1974).

[10] I. Naumov, A. M. Bratkovsky, and V. Ranjan, Unusual Flexoelectric Effect in Two-Dimensional Noncentrosymmetric sp^2-Bonded Crystals, Phys. Rev. Lett. **102**, 217601 (2009).

[11] L. J. Gibson, M. F. Ashby, G. S. Schajer, and C. I. Robertson, The mechanics of two dimensional cellular solids, Proc. R. Soc. A **382**, 25 (1982).

[12] A. Askar and A. S. Cakmak, A structural model of a micropolar continuum, Int. J. Eng. Sci. **6**, 583 (1968).

[13] T. Tauchert, A lattice theory for representation of thermoelastic composite materials, Recent Adv. Eng. Sci. **5**, 325 (1970).

[14] G. Adomeit, in *Mechanics of Generalized Continua*, edited by E. Kröner (Springer, Berlin, 1967).

[15] R. D. Gauthier and W. E. Jahsman, A quest for micropolar elastic constants, J. Appl. Mech. **42**, 369 (1975).

[16] D. Bigoni and W. J. Drugan, Analytical derivation of Cosserat moduli via homogenization of heterogeneous elastic materials, J. Appl. Mech. **74**, 741 (2007).

[17] R. S. Lakes, Experimental microelasticity of two porous solids, Int. J. Solids Struct. **22**, 55 (1986).

[18] A. Merkel and V. Tournat, Experimental Evidence of Rotational Elastic Waves in Granular Phononic Crystals, Phys. Rev. Lett. **107**, 225502 (2011).

[19] R. D. Mindlin, Effect of couple stresses on stress concentrations, Exp. Mech. **3**, 1 (1963).

[20] W. B. Anderson and R. S. Lakes, Size effects due to Cosserat elasticity and surface damage in closed-cell polymethacrylimide foam, J. Mater. Sci. **29**, 6413 (1994).

[21] T. Lee, R. S. Lakes, and A. Lal, Resonant ultrasound spectroscopy for measurement of mechanical damping: Comparison with broadband viscoelastic spectroscopy, Rev. Sci. Instrum. **71**, 2855 (2000).

[22] S. G. Lekhnitskii, *Theory of Elasticity of an Anisotropic Body* (Mir Publishing, Moscow, 1981).

[23] L. Brillouin, *Wave Propagation in Periodic Structures* (Dover Publications, New York, 1953).

[24] A. Spadoni and M. Ruzzene, Elasto-static micropolar behavior of a chiral auxetic lattice, J. Mech. Phys. Solids **60**, 156 (2012).

[25] Z. Rueger and R. S. Lakes, Experimental Cosserat elasticity in open cell polymer foam, Philos. Mag. **96**, 93 (2016).

[26] Z. Rueger and R. S. Lakes, Cosserat elasticity of negative Poisson's ratio foam: Experiment, Smart Mater. Struct. **25**, 054004 (2016).

[27] R. S. Lakes, Foam structures with a negative Poisson's ratio, Science **235**, 1038 (1987).

[28] R. S. Lakes, Materials with structural hierarchy, Nature (London) **361**, 511 (1993).

[29] D. Rayneau-Kirkhope, Y. Mao, and R. Farr, Ultralight Fractal Structures from Hollow Tubes, Phys. Rev. Lett. **109**, 204301 (2012).

[30] C. Kern, M. Kadic, and M. Wegener, Experimental Evidence for Sign Reversal of the Hall Coefficient in Three-Dimensional Metamaterials, Phys. Rev. Lett. **118**, 016601 (2017).

[31] R. D. Mindlin, Micro-structure in linear elasticity, Arch. Ration. Mech. Anal. **16**, 51 (1964).

[32] A. C. Eringen, *Microcontinuum Field Theories, I* (Springer, New York, 1998).